# Bacterial endosymbionts influence fungal transcriptional profiles with implications for host response in the human fungal pathogens *Rhizopus microsporus* and *Rhizopus delemar*

Poppy Sephton-Clark[1], José F Muñoz[2], Herbert Itabangi[1], Kerstin Voelz[1], Christina A Cuomo[2], Elizabeth R Ballou[1]*

[1]*Institute of Microbiology and Infection, School of Biosciences, University of Birmingham, Edgbaston, Birmingham, B15 2TT, UK*

[2]*Infectious Disease and Microbiome Program, Broad Institute of MIT and Harvard, Cambridge, Massachusetts, USA*

***** To whom correspondence should be addressed

ERB: e.r.ballou@bham.ac.uk

**Author contributions**

PSC conceived and designed the experiments, collected the data, performed the analysis and interpretation, and wrote the manuscript.

JFM, HI, KV and CAC contributed to interpretation of the data, and contributed to the manuscript.

ERB conceived and designed the experiments, contributed to interpretation of the data, and wrote the manuscript.

**Funding**

PSC was supported by a BBSRC MIBTP PhD Studentship (BB/M01116X/1). This work was supported by a Wellcome Trust Seed award to KV (108387/Z/15/Z). HI was supported by the Wellcome Trust Strategic Award in Medical Mycology and Fungal Immunology (097377). CAC and JFM were funded by the National Institute of Allergy and Infectious Diseases, National Institutes of Health, under award U19AI110818 to the Broad Institute. ERB was supported by the UK Biotechnology and Biological Research Council (BB/M014525/1) and a Sir Henry Dale Fellowship jointly funded by the Wellcome Trust and the Royal Society (211241/Z/18/Z).

**Abstract**

Mucorales spores, the causative agents of mucormycosis, interact with the innate immune system to cause acute, chronic, or resolving infection. Understanding the factors that influence disease initiation and progression is key to understanding mucormycosis and developing new treatments. Complicating this, mucormycosis can be caused by a number of species that span the Mucorales order and may be host to bacterial endosymbionts. This study sets out to examine the differences between two species in the Mucorales order by characterising their differential interactions with the innate immune system, and their interactions with environmental bacterial endosymbionts. Through a holistic approach, this study examines the transcriptional responses of *Rhizopus delemar* and *Rhizopus microsporus*, two of the most commonly diagnosed species, to innate immune cells. This study also examines the immune cell response and assesses the variation in these responses, given the presence or absence of bacterial endosymbionts within the fungi. We see that the fungal response is driven by interaction with innate immune cells. Moreover, the effect of the bacterial endosymbiont on the fungus is species-specific and strongly influences fungal transcription during phagocyte stress. The macrophage response varies depending on the infecting fungal species, and depending on endosymbiont status. Macrophages are better able to survive when germination is inhibited, or upon a pro-inflammatory response. This work reveals species-specific host responses to related Mucorales spores and shows that bacterial endosymbionts have an important role to play by impacting both innate immune cell response, and fungal response when under stress.

54 **Introduction**

55 Mucormycosis is a devastating, environmentally acquired fungal infection caused by a variety
56 of Mucorales species. Understanding the interaction between Mucorales spores and innate
57 immune cells is key to understanding mucormycosis. Studies frequently focus upon the
58 interaction of a single species of the Mucorales order with innate immune cells (Warris *et al.*
59 2005; Chamilos *et al.* 2008; Schmidt *et al.* 2013; Kraibooj *et al.* 2014; Inglesfield *et al.* 2018).
60 However, between Mucorales species, and across infecting isolates, numerous phenotypic
61 and genomic differences can be observed (Hoffmann *et al.* 2013; Mendoza *et al.* 2014;
62 Schwartze *et al.* 2014), and the range of virulence profiles displayed across the family
63 indicates there may be diversified mechanisms at work (Petraitis *et al.* 2013). Pathogenicity
64 of these species has been linked to the variable copy number of CotH, a family of cell surface
65 proteins important for spores' interactions with and adherence to endothelial cells. Iron-
66 scavenging and melanisation pathways have also been shown to play a role in pathogenicity
67 (Chibucos *et al.* 2016; Andrianaki *et al.* 2018). In addition to fungal genome plasticity and
68 transcriptional responses to host stimuli, fungal-host interactions can be further modulated
69 by bacterial endosymbionts. Endosymbionts have been shown to produce secondary
70 metabolites that modulate pathogenesis, and can directly influence fungal transcription
71 (Partida-Martinez & Hertweck 2005; Itabangi *et al.* 2019; Carter *et al.* 2020). The majority of
72 Mucorales species harbour bacterial endosymbionts, and species can vary between isolates
73 of the same fungal host (Ibrahim *et al.* 2008; Kobayashi & Crouch 2009; Mondo *et al.* 2017;
74 Itabangi *et al.* 2019). For example, *R. microsporus* has been shown to harbour and be
75 modulated by interaction with *Mycetohabitans endofungorum* and *Mycetohabitan*
76 *rhizoxinica* (formerly *Burkholderia endofungorum* and *Burkholderia rhizoxinica)* (Partida-
77 Martinez & Hertweck 2005; Estrada-de los Santos *et al.* 2018). We have recently shown that

78 a bacterial endosymbiont, *Ralstonia pickettii,* influences the outcome of *Rhizopus*
79 *microsporus* infections in both zebrafish and murine models through modulation of both
80 fungal and phagocyte phenotypes (Itabangi *et al.* 2019). However, the impact of this
81 endosymbiont on fungal and host transcriptional responses, and the relevance of
82 endosymbiosis to fungal-mammalian host interactions across Mucorales species, remains
83 uncharacterised.
84
85 Within the Mucorales order, *Rhizopus delemar* and *Rhizopus microsporus* are responsible for
86 the majority of infections within immune compromised individuals (Liu *et al.* 2018). Risk
87 factors for developing the disease include, but are not limited to: innate immune cell
88 deficiencies, uncontrolled diabetes, immune suppression, skin barrier breaches and iron
89 overload (Baldin and Ibrahim 2017). With limited antifungal treatments effective against
90 these invasive infections, there is often a need for surgical debridement or amputation
91 (Spellberg *et al.* 2005). In disseminated cases, mucormycosis may present with a mortality
92 rate of over 90% (Mendoza *et al.* 2014). Reports of chronic mucormycosis have also emerged,
93 affecting both immunocompromised and immunocompetent patients (Alan 2019).
94
95 The innate immune response to Mucorales spores is key to infection control: macrophages
96 are required to induce a differential immune response on contact with *Rhizopus* spp. and, in
97 healthy individuals, may inhibit germination or kill hyphal forms upon contact (Ghuman and
98 Voelz 2017, Andrianaki *et al.* 2018). Host-mediated iron limitation allows macrophages to
99 more effectively kill *Rhizopus* spp. (Ibrahim *et al.* 2008; Liu *et al.* 2015; Andrianaki *et al.* 2018).
100 Single and multi-species studies have shown that phagosome maturation is arrested by
101 melanin within the cell walls of *Aspergillus* spp. and *Rhizopus* spp., and several works

102 comparing *Aspergillus* spp. to *Rhizopus* spp. have revealed similar immunostimulatory
103 capacities, but differences in their responses to host stress (Warris *et al.* 2005; Chamilos *et al.*
104 2008; Schmidt *et al.* 2013; Kraibooj *et al.* 2014). Exploring and understanding fungal responses
105 to the host is essential to improving our understanding of mucormycosis, yet it remains
106 unclear how Mucorales species respond to, and interact with, the innate immune system, and
107 to what extent this varies by species and by holo-genome.
108
109 Our work explores the interplay between the innate immune system, *R. delemar,* and *R.*
110 *microsporus*, and their respective endosymbionts. We investigate the differences between
111 these two fungal species, how they respond transcriptionally to innate immune cells, and how
112 their respective bacterial endosymbionts affect this interaction. We also investigate the
113 transcriptional response of innate immune cells to these infectious spores and determine how
114 this interaction is influenced by the presence of an endosymbiont. We reveal a large
115 difference between the fungal transcriptional profiles of *R. delemar* and *R. microsporus* during
116 *in vitro* monoculture. There is a small conserved response on exposure to innate immune
117 cells, including key changes in cell wall genes, consistent with germination. Conversely, we
118 see that the immune cell response differs significantly between fungal species and is also
119 influenced by the presence or lack of an endosymbiont. We also observe that through the
120 activation of innate immune cells, or upon inhibition of chitin synthase, we can improve the
121 ability of innate immune cells to control fungal spores. Our work represents a broad analysis
122 of the transcriptional interplay between innate immune responders, infectious Mucorales
123 spores, and their respective endosymbionts, revealing species-species differences which
124 question the current model of 'one species represents all', when it comes to mucormycosis.
125

126 **Materials and Methods**

127 Fungal Culture

128 *R. delemar RA 99-880* and *R. microsporus FP469* were cultured with sabouraud dextrose agar
129 (SDA) or broth (SAB) (10 g/liter mycological peptone, 20 g/liter dextrose), sourced from
130 Sigma-Aldrich, at room temperature. Spores were harvested, 10 days after plating, with
131 phosphate-buffered saline (PBS), centrifuged for 3 min at 3,000 rpm, and washed.
132 Appropriate concentrations of spores were used for further experiments as indicated. To cure
133 spores of their respective bacterial endosymbionts, spores treated with ciprofloxacin were
134 germinated, passaged through sporulation twice, and frozen down for stocks before use
135 (Itabangi *et al.* 2019). Successful curing was confirmed by staining and live cell imaging, as
136 described by Itabangi *et al.* Once cured, spores were subcultured at least twice in
137 ciprofloxacin-free media before use. Strains used in this study are identical to those used by
138 Itabangi *et al.* (Itabangi *et al.* 2019) and Ibrahim *et al.* (Ibrahim *et al.* 2008).

139 Macrophage Culture

140 Macrophages from the J774.A1 cell line were cultured in Dulbecco's Modified Eagle Medium,
141 (complemented with 10% foetal bovine serum, 1% penicillin, 1% streptomycin and 1% L-
142 glutamine). Macrophages were routinely grown at 37°C, in 5% $CO_2$.

143

144 Phagocytosis Assay

145 Macrophages were incubated for one hour in serum-free DMEM (sfDMEM) prior to infection.
146 Spores were pre-swollen in SAB (2 hr for *R. delemar,* 4 hr for *R. microsporus*). Washed spores
147 were incubated at a 5:1 multiplicity of infection (MOI) with 1 x $10^5$ macrophages as described
148 in Itabangi *et al.* to ensure that >95% of macrophages contained one spore or more. After a 1

149 hour incubation, excess spores were washed off the surface and the macrophages were
150 incubated for a further 2 hours, before processing for RNA-Seq experiments. For live cell
151 imaging experiments, images were acquired starting immediately after the excess spores
152 were removed.
153
154 Live Cell Imaging
155 Time course images were taken to determine how LPS pre-treatment (100ng/ml) of
156 macrophages, and Nikkomycin Z pre-treatment (24ug/ml over the course of swelling in SAB)
157 of spores effected phagocytic outcome (Mosser and Zhang 2008). Images were acquired at
158 20x on a Zeiss Axio Observer, with imaging every 5 minutes. Bright-field and fluorescent
159 images were then analysed for physical lysis using ImageJ V1. Macrophage survival was
160 determined via analysis of the resulting images.
161
162 Genome Sequencing
163 To confirm the identity of *R. microsporus* (FP469-12.6652333, isolated at the Queen Elizabeth
164 Hospital Birmingham Trauma Centre), DNA was extracted from germinated *R. microsporus*
165 spores following to DNeasy guidelines (Qiagen). Library preparation followed Nextera
166 protocols, and MicrobesNG performed sequencing, utilising an illumina sequencing platform
167 to achieve 30X coverage. The resulting reads were aligned to the indexed genome of *Rhizopus*
168 *microsporus* (ATCC 52813, accession: GCA_002708625.1).
169
170 Comparative Genomics and Enrichment Analysis
171 Fishers exact test was used to detect enrichment of Pfam terms between *R. delemar* and *R.*
172 *microsporus*, terms with a corrected P value of < 0.01 were considered significant. Orthologue

173 genes of *R. delemar* and *R. microsporus* were identified using blast+. R (version 3.3.3) was
174 used to carry out hypergeometric testing of KEGG and GO terms to determine enrichment.
175
176 Bacterial RNA-Seq
177 Transcriptional analysis of *R. pickettii* was assessed following growth for 4 h at 30 °C, 80-150
178 rpm in DMEM, or DMEM + cured *R. microsporus* hyphae. Triplicate biological replicates were
179 prepared for each condition. RNA was extracted using the modified Qiagen RNA extraction
180 method. Briefly, TRIzol was used to lyse the samples, which were then either immediately
181 frozen at −20°C and stored for RNA extraction or placed on ice for RNA extraction. After lysis,
182 0.2 ml of chloroform was added for every 1 ml of TRIzol. Samples were incubated for 3 min,
183 then spun at 12,000 g at 4°C for 15 min. To the aqueous phase, an equal volume of 100%
184 ethanol (EtOH) was added, before the samples were loaded onto RNeasy RNA extraction
185 columns (Qiagen). The manufacturer's instructions were followed from this point onwards.
186 RNA quality was checked by Agilent, with all RNA integrity number (RIN) scores above 7. One
187 microgram of total RNA was used for cDNA library preparation. Library preparation was done
188 in accordance with the NEBNext pipeline, with libraries quality checked by Agilent. Samples
189 were sequenced using the Illumina NextSeq platform; 150-bp paired-end sequencing was
190 employed (2 x 150 bp) (>10 million reads per sample). The output was aligned to the *R.*
191 *pickettii* 12J reference with Hisat2 (Version 2.0.5), and downstream analysis was performed
192 with HTSeq (Version 0.10.0) and edgeR (Version 3.16.5).
193
194 Fungal RNA-Seq
195 RNA was extracted from spores which had either been incubated with the macrophages, or
196 incubated in DMEM for the equivalent time period (3 biological replicates per condition). To

197 remove the macrophages, triton at 1% was used to lyse the macrophages, the resulting
198 solution was then centrifuged for 3 min at 3,000 rpm, and washed, leaving only spores. The
199 DMEM control also received the same treatment. To extract total RNA, the washed samples
200 were immediately immersed in TRIzol and lysed via bead beating at 6,500rpm for 60s.
201 Samples were then either immediately frozen at -20°C and stored for RNA extraction or
202 placed on ice for RNA extraction. After lysis, 0.2 ml of chloroform was added for every 1 ml of
203 TRIzol used in the sample preparation. Samples were incubated for 3 min and then spun at
204 12,000 *g* at 4°C for 15 min. To the aqueous phase, an equal volume of 100% ethanol (EtOH)
205 was added, before the samples were loaded onto RNeasy RNA extraction columns (Qiagen).
206 The manufacturer's instructions were followed from this point onwards. RNA quality was
207 checked by Agilent, with all RNA integrity number (RIN) scores above 7 (Schroeder *et al.*
208 2006). One microgram of total RNA was used for cDNA library preparation. Library
209 preparation was done in accordance with the NEBNext pipeline, with library quality checked
210 by Agilent. Samples were sequenced using the Illumina HiSeq platform; 100-bp paired-end
211 sequencing was employed (2 x 100 bp) (>10 million reads per sample).

212 Single Cell RNA-Seq

213 For single cell sequencing experiments, macrophages were infected with fungal spores, as
214 outlined above. Uninfected macrophages, used as a negative control, were treated in the
215 same manner and underwent mock washes and media changes at identical time points to
216 infected macrophages. Macrophages were isolated and released from the bottom of their
217 wells with accutase, as per manufacturer's instructions (Technologies n.d.). Once in solution,
218 the macrophages were loaded onto the 10X genomics single cell RNA sequencing pipeline for

219 single cell isolation and library preparation. In total, 1082 single cells were sequenced. The
220 libraries were sequenced on the Illumina Sequencing Platform.
221
222 Data Analysis
223 For the fungal and bacterial RNA-Seq data, FastQC (version 0.11.5) was employed to ensure
224 the quality of all samples. Hisat2 (version 2.0.5) was used to align reads to the indexed
225 genome of *Rhizopus delemar* RA 99-880 and the indexed genome of *Rhizopus microsporus*
226 (ATCC 52813, accession: GCA_002708625.1) (Ma *et al.* 2009; Mondo *et al.* 2017). HTSeq
227 (version 0.8.0) was used to quantify the output (Anders *et al.* 2015). Trinity and edgeR (version
228 3.16.5) were then used to analyse differential expression (Robinson *et al.* 2010; Grabherr *et*
229 *al.* 2011). For the single cell RNA-Seq data, the 10X genomics analysis pipeline (Loupe Cell
230 Browser V 2.0.0, Cell Ranger Version V 2.0.0) was used to align reads to the *mus musculus*
231 genome (version MM10), and quantify the output. For single cell analysis, the samples were
232 then aggregated using the 10X genomics analysis pipeline, to allow comparisons between
233 samples.

234 **Data Availability**

235 Data have been uploaded to the SRA database and can be accessed via the following accession
236 numbers: PRJNA680574 (*R. microsporus*), PRJNA680572 (*R. delemar*), PRJNA680577 (*R.*
237 *pickettii*), PRJNA680578 (macrophage).
238
239

240 **Results**

241 *Experimental Design*

242 We set out to investigate paired transcriptional responses of host and fungal cells, whilst also
243 exploring the influence of the endosymbiont on this interaction (Figure 1a). Fungal spores
244 from *Rhizopus delemar* and *Rhizopus microsporus* were either cured via ciprofloxacin
245 treatment to remove the bacterial endosymbiont (cured) or maintained in media permissive
246 to bacterial endosymbiosis (wt). Cured spores were passaged twice in the absence of
247 ciprofloxacin to limit the impact of the drug on transcriptional responses. The cured and wt
248 spores of both *R. delemar* and *R. microsporus* were allowed to swell in sabouraud broth (SAB)
249 until 95% of the population had reached mid isotropic phase. Due to the differences in
250 germination rates between the species (Figure 1b), this occurred at 2 hours for *R. delemar*
251 and 4 hours for *R. microsporus.* Swollen spores were then used to infect the J774.1 murine
252 macrophage-like cell line. Fungal spores were co-cultured with macrophages for one hour,
253 after which unengulfed spores were removed, and phagocytosed spores were incubated
254 within the macrophages for a further two hours. The cells from the resulting infection were
255 processed to explore their transcriptional response to this infection scenario (Figure 1a).
256 Macrophages that had phagocytosed fungal spores were isolated and sequenced via the 10X
257 Genomics Chromium Single Cell Sequencing platform. Macrophages left unexposed to the
258 fungi were used as a negative control. RNA was also isolated from fungal spores (cured and
259 wt) which had been engulfed by macrophages, and this was sequenced with a bulk RNA-Seq
260 approach. Unexposed fungi (cured and wt) were incubated in macrophage media for a
261 matched time and used as a negative control. The resulting data shows the fungal response
262 to phagocytosis by macrophages, as well as the fungal response to the presence of its
263 endosymbiont (Figures 2-5). The macrophage response to the two species is also revealed, a

264 response which appears to differ when the endosymbiont is present for both fungal species
265 (Figures 6-7).
266
267 *Comparative genomics of Rhizopus species*
268 In order to better understand differential disease progression in mucormycosis, we chose to
269 compare *R. delemar* and *R. microsporus*, as they cause a large proportion of mucormycosis
270 infections but appear morphologically dissimilar. *R. delemar* germinates more quickly than *R.*
271 *microsporus*, with 50% of spores germinating by 3 hours, and a mean spore body size which
272 reaches 12.8 μm over the course of germination (Figure 1b, c). *R. microsporus* germinates at
273 a significantly slower rate, taking 6 hours for 50% of spores to germinate, with a final mean
274 spore body size of 13.9 μm (Figure 1b, c). To better understand their relationship to one
275 another, we compared the gene content of the two species to explore the similarity and
276 differences between them. Previous work has established that the *R. delemar* genome (45.3
277 Mb, 17,513 genes) is larger, and contains an increased number of genes, compared to the *R.*
278 *microsporus* genome (26 Mb, 10,959 genes) (Ma *et al.* 2009; Mondo *et al.* 2017). Our results
279 show that, compared to *R. microsporus*, the genome of *R. delemar* is enriched for genes with
280 protein domains (PFAM) associated with ion binding, carbohydrate derivative binding, nucleic
281 acid binding, cytoskeletal protein binding, poly(A) binding, NAD+ ADP-ribosyltransferase
282 activity, protein kinase C activity, translation initiation factor binding and inorganic phosphate
283 transmembrane transporter activity (Supplemental Figure 1, Figure 1d). *R. microsporus* is
284 enriched for genes with protein domains corresponding to nucleoside phosphate binding,
285 early endosome activity and DNA repair complex activity (Supplemental Figure 1, Figure 1d).
286 The clear differences illustrated by genome size and gene content indicate the likelihood of
287 alternative transcriptional responses.

288

289 *Alternative transcriptional profiles are presented by R. delemar and R. microsporus in response*
290 *to innate immune cells*

291 First, we examined overall trends in fungal responses to phagocytosis, obtained through our
292 bulk RNA-Seq approach. We analysed the signal obtained from *R. delemar* and *R. microsporus*
293 samples with principle component analysis (PCA) (Figure 2). We observed large differences
294 between the transcriptomes of both fungal species, when exposed or unexposed to
295 macrophages, while the presence or absence of their respective endosymbionts had a weak
296 but differential effect on PCA. The presence or absence of the endosymbiont appears to have
297 very little bearing on the transcriptional patterns displayed by *R. delemar*, as samples fell into
298 two distinct clusters, most strongly influenced by macrophage exposure (Figure 2a). *R.*
299 *microsporus* exhibits a similar trend upon exposure to macrophages, however the presence
300 of the endosymbiont also influenced clustering (Figure 2b). Here, we focus on the
301 transcriptional analysis of the host-pathogen-endosymbiont interaction across the two
302 species.

303

304 There are 2,493 genes that are significantly differentially expressed (Log fold change > 2; false
305 discovery rate < 0.05) in *R. delemar* across all conditions (Figure 3a), while *R. microsporus* only
306 exhibits 40 genes significantly differentially expressed across all conditions (Log fold change
307 > 2; false discovery rate < 0.05) (Figure 3b). The theme of a muted transcriptional response
308 from *R. microsporus* is also seen within pairwise comparisons of conditions. Pairwise
309 comparisons of differential expression across each experimental condition show similar
310 trends in responses between *R. delemar* and *R. microsporus*, however *R. microsporus*
311 responds with a reduced gene set (Figure 4). Pairwise comparisons showed the biggest shift

312 in transcriptional response is observed when comparing phagocytosed fungal spores to those
313 unexposed to macrophages, regardless of endosymbiont status. When phagocytosed
314 (Supplemental Figure 2), *R. microsporus* upregulates genes enriched in GO categories
315 corresponding to thiamine metabolism, sulfur metabolism, glycerol metabolism, alcohol
316 dehydrogenase activity and transmembrane transporter activity (hypergeometric test,
317 corrected *P* value < 0.05). This is consistent with the fungal response seen to macrophage
318 stress, and the micronutrient scavenging response to nutritional immunity (Parente-Rocha *et*
319 *al.* 2015; Ballou and Wilson 2016; Andrianaki *et al.* 2018; Shen *et al.* 2018). Phagocytosed *R.*
320 *microsporus* downregulated genes enriched in GO categories corresponding to rRNA
321 processing, ribosome biogenesis and ribosome localization (hypergeometric test, corrected *P*
322 value < 0.05) (Supplemental Figure 2), consistent with growth arrest within the
323 phagolysosome (Andrianaki *et al.* 2018; Inglesfield *et al.* 2018).
324
325 Comparisons of *R. delemar* conditions reveal that, upon phagocytosis, spores upregulate
326 genes enriched in KEGG classifications corresponding to MAPK signalling, phenylalanine
327 metabolism, tyrosine metabolism, glutathione metabolism and fatty acid synthesis
328 (hypergeometric test, corrected *P* value < 0.05). Upregulation of these processes is consistent
329 with melanin biosynthesis and intra-phagosomal survival (Lorenz and Fink 2001; Yadav *et al.*
330 2011; Eisenman and Casadevall 2012; Andrianaki *et al.* 2018). Unexposed *R. delemar* spores
331 upregulate genes enriched in KEGG classifications corresponding to ketone body synthesis,
332 protein processing via the endoplasmic reticulum, amino sugar and nucleotide sugar
333 metabolism (hypergeometric test, corrected *P* value < 0.05). This is consistent with metabolic
334 activation and cell wall biogenesis (Figure 5).
335

336 *R. delemar and R. microsporus transcriptional responses to innate immune cells are impacted*
337 *by loss of endosymbionts*
338 *R. delemar* and *R. microsporus* harbour distinct bacterial endosymbionts (Itabangi *et al.* 2019;
339 Ibrahim *et al.* 2008). The endosymbiont of *R. microsporus* was isolated and identified as
340 *Ralstonia pickettii*, and presence of an unculturable *R. delemar* endosymbiont previously
341 reported by Ibrahim *et al.* was confirmed with PCR (Itabangi *et al.* 2019; Ibrahim *et al.* 2008,
342 data not shown). When comparing transcriptional profiles of wt and cured spores incubated
343 in serum-free DMEM (sfDMEM) for 3 hours (time matched to phagocytosis assay), we
344 observed very few transcriptional changes in either fungal species in response to curing
345 (Supplemental Table 1). In *R. delemar,* a single gene, predicted to be a putative protein
346 phosphatase, was repressed. In *R. microsporus,* three genes were induced: an autophagy-
347 related protein, a C2H2 zinc finger transcription factor, and ribosomal protein L2. In contrast,
348 loss of the endosymbiont significantly impacted the transcriptional responses of both fungal
349 species to macrophages (Figure 4). Specifically, we observed an overall increase in the
350 number of fungal genes differentially regulated upon phagocytosis for both species.
351
352 Exposure of wt *R. microsporus* to macrophages induced the expression of one gene with no
353 known function and repressed 6 genes. The repressed genes include an autophagy-related
354 protein and a zinc finger transcription factor, as well as 4 un-annotated genes (Figure 4,
355 Supplemental Table 1). In contrast, when cured *R. microsporus* spores were exposed to
356 macrophages, 277 genes were significantly induced and 82 repressed, compared to
357 unexposed cured spores (Figure 4). Induced genes were enriched (hypergeometric test,
358 corrected $P$ value $< 0.05$) for the following GO categories: organelle organisation, pre-
359 ribosome and ribosome activity, ATPase activity, hydrolase activity, pyrophosphatase activity,

360 helicase activity, nucleic acid binding, RNA metabolism, nitrogen metabolism, chromatin
361 silencing. Repressed genes were enriched (hypergeometric test, corrected *P* value < 0.05) for
362 the following GO categories: oxidoreductase activity, hydrogen sulphide metabolism,
363 glycolysis, sulphur metabolism, hexose catabolism, siderophore activity, iron assimilation,
364 nitrogen metabolism, carboxylic acid metabolism. This suggests an overall failure to properly
365 respond to host stresses such as iron starvation in the absence of the bacterial endosymbiont.
366 Itabangi *et al.* have shown that the presence of the endosymbiont *Ralstonia pickettii* impacts
367 resistance to host-relevant stress and pathogenesis, and this is reflected in the transcriptional
368 changes observed here (Itabangi *et al.* 2019).
369
370 A similar impact of the unidentified endosymbiont was observed for *R. delemar.* In wt
371 samples, the overall fungal response to phagocytosis is characterized by a robust
372 transcriptional response: induced genes in wt samples (1137 genes, Figure 4) were enriched
373 for KEGG classifications corresponding to: alanine metabolism, PPAR signalling, aromatic
374 compound biosynthesis and degradation, lysine metabolism, lipid metabolism, MAPK
375 signalling, sugar metabolism, tyrosine metabolism, secondary metabolite biosynthesis (Figure
376 5). Repressed genes in wt samples (472 genes, Figure 4) were enriched for KEGG
377 classifications corresponding to: carbohydrate metabolism, secondary metabolite
378 biosynthesis, ketone body processing, protein processes, MAPK signalling (Figure 5). In
379 contrast, induced genes in cured samples (1285 genes, Figure 4) were enriched for KEGG
380 classifications corresponding to: Fatty acid metabolism, DNA replication, amino acid
381 metabolism, glycan metabolism, pyruvate metabolism, secondary metabolite processing
382 (Figure 5). Repressed genes in cured samples (878 genes, Figure 4) were enriched for KEGG
383 classifications corresponding to: sugar metabolism, amino acid metabolism, lipid metabolism,

384 MAPK signalling, NOD-like receptor signalling. Again, this suggests that the endosymbiont has
385 an overall suppressive impact on fungal transcription in response to macrophage challenge.
386
387 *R. delemar and R. microsporus exhibit distinct transcriptional profiles with implications for*
388 *virulence*
389 Next, we directly compared the transcriptional patterns of genes shared across the two fungal
390 species. When comparing the transcriptional responses of orthologous genes shared by *R.*
391 *delemar* and *R. microsporus*, we saw only a small proportion behave similarly (213 genes).
392 When phagocytosed, wt spores from both species upregulate orthologues genes involved in
393 fatty acid catabolism, transcription, regulation via polymerase II, and organelle organization.
394 Phagocytosed cured spores from both species upregulate orthologous genes involved in RNA
395 processing, chromosome organization and condensed chromosome pathways. When
396 unexposed, we see wt spores upregulate orthologous genes involved in translocation, protein
397 binding, siderophore activity, cobalmin processing, and post-translational protein targeting.
398 Cured unexposed spores upregulate orthologous genes with roles in siderophore activity and
399 transferase activity. Overall, *R. delemar* and *R. microsporus* both respond transcriptionally to
400 the presence of macrophages, however the size and composition of this response differs
401 between species. This may reflect the accommodation of different endosymbiont species, as
402 well as the differences in genome size and structure between *R. delemar* and *R. microsporus*.
403
404 Finally, we examined the regulation of genes predicted to be involved in ferrous iron
405 transport, as previous work has linked iron scavenging to survival within the phagolysosome
406 (Andrianaki *et al.* 2018). There are 12 genes in the *R. delemar* genome with predicted ferrous
407 iron roles. While 8 showed no significant change over the tested conditions, 3 (R0G3_006623,

408 R0G3_007727, R0G3_011864) appeared highly expressed in wt and cured phagocytosed
409 spores, compared to unexposed spores. The last gene, ROG3_009943, is highly expressed in
410 wt spores unexposed to macrophages. Together, this suggests there may be condition
411 dependent specialization in the expression of ferrous iron transport in *R. delemar*.
412
413 *Ralstonia pickettii upregulates fatty acid metabolism and transport in the presence of R.*
414 *microsporus*
415 To identify the response of *R. microsporus*' bacterial endosymbiont to its fungal host, we
416 analysed transcription of *R. pickettii* isolated from *R. microsporus* in the following conditions:
417 DMEM, and DMEM supplemented with *R. microsporus* substrate (heat killed cured
418 mycelium). When grown in the absence of *R. microsporus* substrate, functions including
419 oxidative phosphorylation, 4Fe-4S binding, heat shock response (HSP20) and cytochrome c
420 activity were upregulated. When supplemented with fungal substrate, an increase in fatty
421 acid metabolism, Acyl-CoA activity, ABC transporter activity and tetR regulation arises,
422 suggestive of fungal substrate use for metabolic processes (Supplemental Figure 3).
423
424 *Innate immune cell transcription varies with fungal species and endosymbiont presence*
425 To investigate the innate immune response when challenged with *R. delemar* and *R.*
426 *microsporus*, we carried out single cell RNA-Seq of J774.A1 murine macrophages, unexposed
427 and exposed for 3 hours to the four types of pre-swollen spores (Figure 1a). Both challenged
428 and unchallenged macrophages separate based on challenge status when DEGs (adjusted $P <$
429 $0.0001$) are used to determine principal components (Supplemental Figure 4a). Enrichment
430 analysis of all DEGs identifies that other than challenge status (Supplemental Figure 4a, PC2)
431 cells strongly differentiate based on cell cycle (Supplemental Figure 4b, PC1). Enrichment

432 analysis of all DEGs identifies the most highly enriched functions to be cell cycle, carbohydrate
433 metabolism, cell signalling, and protein turnover (Supplemental Figure 4b). To identify the
434 transcriptional patterns of genes responding to the spores, we focused on the expression of
435 a subset of genes previously identified as immune response genes (Munoz *et al.* 2018).
436 Principle component analysis of the aggregated transcriptional data supports there is a clear
437 difference in transcription between macrophages that have and have not been exposed to
438 the fungi (Figure 6). Across all exposed conditions, relative to unexposed macrophages, there
439 was a profile consistent with cytokine activation, response to stimulus, and activation of the
440 NF-Kb pathway. This was accompanied by repression of CCL5, which is involved in T-cell
441 recruitment (Figure 7). However, different macrophage profiles can be seen in response to
442 the two fungal species, and these are further influenced by the presence of the
443 endosymbiont. While the response to wt *R. delemar* shows the most deviation from the
444 macrophage-only control, exposure to cured *R. delemar* also elicited a strong and distinct
445 macrophage response (Figures 6,7). Exposure to wt *R. delemar* elicits increased expression of
446 general markers of activation, including GTPase activity and MHC class II protein binding
447 (LAG3 repressor of T-cell activation, H2-M2, IFN-gamma induced IIGP1, MX1, KCTD14, PNP2),
448 growth factor binding, IL1 receptor agonist activity and endocytosis (SERPINE1, ENG, FGFBP3,
449 GM8898, GCNT2, IL1F6) (Martinez *et al.* 2013; Szulzewsky *et al.* 2015). Specifically, we
450 observe modest increases in the expression of IFN-$\gamma$ responsive CXCL10 (3.1 fold) and
451 IRG1/IRG11 (5.9 fold), pro-inflammatory SAA3 (3.5 fold), and ENPP4 (2.8 fold), but also
452 induction of the M2 polarizing PSTPIP2/21 (6.7 fold), the IL-4 responsive signaling modulator
453 CISH (5.4 fold), and the vascular damage responsive F3/F31 (5.9 fold) (Martinez *et al.* 2013;
454 Ye and Sun 2015). These latter genes are not as strongly induced during exposure to *R.*
455 *microsporus*, which may reflect the aggressive nature of infection by *R. delemar* relative to *R.*

456 *microsporus.* In contrast, infection with cured *R. delemar* showed a decrease in the induction
457 of these M2-polarisation markers (PSTPIP2, 3.5 fold relative to uninduced). The
458 transcriptional profile is instead shifted to include increased transcription of genes involved
459 in G protein signaling and phosphoinositide binding (PDE7B, CCL1, SCARF1, RGS16, PLEKHA4)
460 (Figure 7).
461
462 A similar change in macrophage polarization was observed during exposure to *R. microsporus.*
463 For both wt and cured *R. microsporus,* expression of IFN-$\gamma$ responsive CXCL10, SAA3, and
464 ENPP4 was comparable to unexposed macrophages. Compared to *R. delemar,* exposure to wt
465 *R. microsporus* induced a more limited expression of genes with roles in cytokine activation,
466 ERK1 and ERK2 regulation, and regulation of NF-kB cascade (Figure 7). There was also a
467 weaker induction of the vascular damage responsive F3/F31 genes, and a relatively stronger
468 upregulation of the PLA2G16 phospholipase, TRIM30D, SLC1A2 and the M2 polarizing IL-6
469 (Berger and Hediger 2006; Luckett-Chastain *et al.* 2017; Raggi *et al.* 2017; van Tol *et al.* 2017;
470 Gerrick *et al.* 2018). However, other key polarizing genes, particularly PSTPIP2/21, SAA3, and
471 ENPP4 were only weakly induced (Supplemental Table 2)(Raggi *et al.* 2017). Overall, this
472 profile suggests a weak M1-like activation consistent with poor phagocytosis and reduced
473 overall antifungal activity that we observe in macrophages interacting with endosymbiont-
474 harbouring spores (Itabangi *et al.* 2019).
475
476 Finally, cured *R. microsporus* induced a strong pro-inflammatory response, which included
477 upregulation of CXCL3, the neutrophil chemoattractant, consistent with our observations of
478 differences in phagocyte recruitment in zebrafish upon infection with wt vs. cured spores
479 (Owen and Mohamadzadeh 2013; Hou *et al.* 2014; Itabangi *et al.* 2019). Markers of NF-kB

480 activation were also strongly induced in this population. Cured *R. microsporus* also strongly
481 induced the expression of TNFRSF8 (CD30), a marker of lymphocyte activation occasionally
482 associated with subcutaneous fungal infections (Muller *et al.* 2011). Overall, this is suggestive
483 of a shift to a more pro-inflammatory profile. Itabangi *et al.* observed that cured *R.*
484 *microsporus* is more sensitive to phagocyte-mediated killing and phagocyte recruitment
485 compared to wt (Itabangi *et al.* 2019). We therefore went on to test whether a more
486 successful response to the spores could be mounted via the induction of a pro-inflammatory
487 response.
488
489 *Chitin synthase inhibition and pro-inflammatory priming regulate infection outcome*
490 *R. delemar* exhibits rapid germination followed by hyphal extension (Sephton-Clark *et al.*
491 2018). The transcriptional profile we observe here in macrophages exposed to *R. delemar* is
492 consistent with a strong damage response, likely prompted by the germination of *R. delemar*
493 spores. We therefore hypothesised that macrophages may be better able to control the
494 infection if the fungi were slowed in their developmental progress. The necessity of genes
495 involved in chitin synthesis and regulation appeared important for both *R. delemar* and *R.*
496 *microsporus* in response to phagocytosis (Supplemental Figure 5). In previous work we also
497 highlighted the importance of chitin synthase for germination (Sephton-Clark *et al.* 2018). We
498 therefore tested this model by examining macrophage-fungal interaction following treatment
499 with a chitin synthesis inhibitor. When fungal spores were pre-treated with the chitin
500 synthesis inhibitor Nikkomycin Z (120 μg/ml), both *R. delemar* and *R. microsporus* spores
501 underwent swelling, but failed to germinate, and displayed less chitin/chitosan in their outer
502 cell wall (Supplemental Figure 6). Treatment with lower Nikkomycin Z concentrations (24
503 μg/ml) allowed spores to swell, but development appears halted after swelling, and

504 macrophage survival increases to 7.5 hours post infection (Figure 8). As the macrophages are
505 better able to control these spores, this suggests that spores undergoing the initial stages of
506 germination may offer less of a challenge for the macrophages than those able to polarise
507 and germinate.
508
509 Our transcriptional data show a strong M2 alternative activation signal during *R. delemar*-
510 macrophage interaction, but a weaker M2 polarisation during *R. microsporus*-macrophage
511 interaction that was further shifted towards NF-kB-mediated M1 upon endosymbiont cure.
512 We therefore hypothesized that shifting the macrophage polarization towards M1 classical
513 activation might have a protective effect upon Mucorales infection. Consistent with this, the
514 pre-treatment of macrophages with NF-kB activating lipopolysaccharide (LPS) significantly
515 improved the ability of macrophages to control *R. microsporus* that maintained the
516 endosymbiont. At 7.5 hours post infection, 59.7% of macrophages survived when pre-treated
517 with LPS, compared to 24.6% without (Figure 8).
518
519
520 **Discussion**
521 This work utilises swollen spores to investigate the interplay between *Rhizopus* species and
522 innate immune cells. Previous studies have used either swollen or resting spores to
523 investigate the interaction between Mucorales species and the host (Inglesfield *et al.* 2018;
524 Andrianaki *et al.* 2018). Itabangi *et al.* demonstrate that swollen *R. microsporus* spores show
525 increased virulence when the endosymbiont *R. pickettii* is present, however, cured swollen
526 and cured resting spores are cleared to a similar extent within *in vivo* models (Itabangi *et al.*
527 2019). Furthermore, Mucorales spores swell upon immersion in minimal media (Guo *et al.*

528 1998; Turgeman *et al.* 2013) and likely similarly begin swelling once they are in a host
529 environment. Therefore, understanding the interaction between immune cells and swollen
530 spores is key to understanding pathogenesis. Further transcriptional studies to investigate the
531 differences between interactions of resting and swollen spores with the host would provide
532 useful information on the impact of developmental stage on infection progression.
533
534 Whilst the endosymbiont of *R. microsporus* was cultured and identified as *Ralstonia pickettii*,
535 culturing the endosymbiont of *R. delemar* posed a much larger challenge, and this bacterium
536 ultimately remained unculturable. Further efforts to characterise this endosymbiont would
537 offer unique insights into this species-specific symbiosis. Our model uses innate immune cells
538 cultured *in vitro*. Itabangi et al highlight that similar results are seen when using murine
539 macrophages, amoeba, and multiple *in vivo* models (Itabangi *et al.* 2019), and further *in vivo*
540 work will continue to inform our understanding of Mucorales pathogenesis.
541
542 In this work we show that the fungal response to innate immune cells differs by species in the
543 Rhizopodaceae family. Although *R. delemar* and *R. microsporus* share a small conserved
544 response on exposure to macrophages, the majority of their response differs. We show that
545 the ability to germinate prior to phagocyte control appears to be key to virulence, as blocking
546 spore germination with the chitin synthase inhibitor Nikkomycin Z improves macrophage
547 survival. A range of germination and virulence phenotypes can be seen throughout the
548 Mucorales, and this highlights a need for further investigation into these differences, to better
549 understand the infections they cause.
550

551 We have also shown that the fungal transcriptional response appears largely unperturbed by
552 the presence, or lack, of an endosymbiont, in the absence of stress. However, the presence
553 of an endosymbiont greatly effects the response of and to the host. It has been shown
554 that endosymbionts influence asexual development and sporulation through the regulation
555 of Ras2 (Mondo *et al.* 2017). While we observed limited changes in fungal transcription when
556 comparing wt and cured spores, we did observe changes in the expression of fungal genes
557 upon exposure to macrophages. Itabangi et al show that the endosymbiont of *R. microsporus*
558 enhances virulence through the secretion of an anti-phagocytic factor. The endosymbiont
559 also impacts organisation of the fungal plasma membrane, as well as environmental stress
560 resistance and resistance to macrophage-mediated killing (Itabangi *et al.* 2019). Here, we
561 show that this is mirrored by the transcriptional response of the wt and cured spores of both
562 *Rhizopus* species to macrophages, and in the macrophage response to infection.
563
564 As anticipated, activation of pro-inflammatory pathways increased macrophage survival in
565 response to the spores. This consolidates several studies which demonstrate improved innate
566 immune cell response to fungal pathogens when primed (Blasi *et al.* 1995; Municio *et al.* 2013;
567 Rogers *et al.* 2013). It has been shown that the early immune response to a *Mucor*
568 *circinelloides* infection is dependent on the formation of a pro-inflammatory TNF-$\alpha$-
569 expressing granuloma-like structure that controls but does not kill spores in the zebrafish
570 model (Inglesfield *et al.* 2018). Ungerminated *Rhizopus* spores are highly resistant to
571 ROS/RNS, which may mediate survival within granulomata.
572
573 Interestingly, we see the chitin synthase inhibitor, Nikkomycin Z, is able to inhibit germination
574 in both *R. delemar* and *R. microsporus*. This demonstrates the requirement of chitin synthase

575 for spore development in these species, reflected in our transcriptional analysis. Treated
576 spores remain viable and swell, but do not polarise. The ability to germinate also has
577 consequences for virulence. The ability of macrophages to control swollen spores, but not
578 subsequently polarised ones, highlights that the developmental stage of the spore is key to
579 innate immune success and control. Whilst many fungal pathogens are virulent in an
580 ungerminated form, germination appears a key virulence factor for these filamentous fungi.
581 This is confirmed by work which shows that the developmental stage of *R. microsporus, R.*
582 *delemar* and *Rhizopus oryzae* spores impacts pathogenesis in zebrafish and murine models
583 (Andrianaki *et al.* 2018; Itabangi *et al.* 2019). Specifically, infection with pre-swollen spores
584 leads to evasion of macrophage-mediated immunity and increased pathogenesis (Andrianaki
585 *et al.* 2018; Itabangi *et al.* 2019). In both models, spore clearance is dependent on phagocyte
586 recruitment. In addition, phagocyte recruitment (Itabangi *et al.* 2019) and activation (Figure
587 7) is influenced by endosymbiont status (Andrianaki *et al.* 2018; Itabangi *et al.* 2019). Finally,
588 we extended this analysis by revealing profound differences in the host response to two
589 closely related *Rhizopus* species. In particular, we observe a M2/damage-associated response
590 during infection with wt *R. delemar* spores that is shifted towards an M1 protective response
591 upon infection with cured *R. microsporus* spores. We reinforce this finding through
592 experimental modulation of macrophage polarization, showing that exposure to strongly M1-
593 polarizing LPS is sufficient to reduce macrophage killing by wt *R. delemar* spores. Therefore,
594 our data provide a framework for beginning to understand differences in the relative
595 virulence of pathogenic Mucorales species and underpin our finding of cross-kingdom fungal-
596 bacterial symbiosis influencing mammalian disease.
597
598

**Acknowledgments**

We are grateful to the University of Birmingham's Genomics Services Facility and to Deborah Croom-Carter for her technical support.

**References:**

Alan, E. C. (2019). "An Emergent Entity : Indolent Mucormycosis of the Paranasal Sinuses, A Multicenter Study." **2193**: 92–100.

Anders, S., P. T. Pyl and W. Huber (2015). "HTSeq--a Python framework to work with high-throughput sequencing data." Bioinformatics **31**(2): 166-169.

Andrianaki, A. M., I. Kyrmizi, K. Thanopoulou, C. Baldin, E. Drakos, S. S. M. Soliman, A. C. Shetty, C. McCracken, T. Akoumianaki, K. Stylianou, P. Ioannou, C. Pontikoglou, H. A. Papadaki, M. Tzardi, V. Belle, E. Etienne, A. Beauvais, G. Samonis, D. P. Kontoyiannis, E. Andreakos, V. M. Bruno, A. S. Ibrahim and G. Chamilos (2018). "Author Correction: Iron restriction inside macrophages regulates pulmonary host defense against Rhizopus species." Nat Commun **9**(1): 5015.

Baldin, C. and A. S. Ibrahim (2017). "Molecular mechanisms of mucormycosis-The bitter and the sweet." PLoS Pathog **13**(8): e1006408.

Ballou, E. R. and D. Wilson (2016). "The roles of zinc and copper sensing in fungal pathogenesis." Curr Opin Microbiol **32**: 128-134.

Berger, U. V. and M. A. Hediger (2006). "Distribution of the glutamate transporters GLT-1 (SLC1A2) and GLAST (SLC1A3) in peripheral organs." Anat Embryol (Berl) **211**(6): 595-606.

620 Blasi, E., R. Barluzzi, R. Mazzolla, B. Tancini, S. Saleppico, M. Puliti, L. Pitzurra and F. Bistoni
621 (1995). "Role of nitric oxide and melanogenesis in the accomplishment of anticryptococcal
622 activity by the BV-2 microglial cell line." J Neuroimmunol **58**(1): 111-116.
623 Carter ME, Carpenter SCD, Dubrow ZE, Sabol MR, Rinaldi FC, Lastovetsky OA, Mondo SJ,
624 Pawlowska TE, Bogdanove AJ (2020). "A TAL effector-like protein of an endofungal bacterium
625 increases the stress tolerance and alters the transcriptome of the host." Proc Natl Acad Sci U
626 S A **117**(29):17122–17129.
627 Chamilos, G., R. E. Lewis, G. Lamaris, T. J. Walsh and D. P. Kontoyiannis (2008). "Zygomycetes
628 hyphae trigger an early, robust proinflammatory response in human polymorphonuclear
629 neutrophils through toll-like receptor 2 induction but display relative resistance to oxidative
630 damage." Antimicrob Agents Chemother **52**(2): 722-724.
631 Eisenman, H. C. and A. Casadevall (2012). "Synthesis and assembly of fungal melanin." Appl
632 Microbiol Biotechnol **93**(3): 931-940.
633 Estrada-de los Santos P, Palmer M, Chávez-Ramírez B, Beukes C, Steenkamp ET, Briscoe L,
634 Khan N, Maluk M, Lafos M, Humm E, et al (2018). "Whole genome analyses suggests that
635 Burkholderia sensu lato contains two additional novel genera (Mycetohabitans gen. nov., and
636 Trinickia gen. nov.): Implications for the evolution of diazotrophy and nodulation in the
637 Burkholderiaceae." Genes (Basel) **9**(8):389.
638 Gerrick, K. Y., E. R. Gerrick, A. Gupta, S. J. Wheelan, S. Yegnasubramanian and E. M. Jaffee
639 (2018). "Transcriptional profiling identifies novel regulators of macrophage polarization."
640 PLoS One **13**(12): e0208602.
641 Ghuman, H. and K. Voelz (2017). "Innate and Adaptive Immunity to Mucorales." J Fungi (Basel)
642 **3**(3).

643 Grabherr, M. G., B. J. Haas, M. Yassour, J. Z. Levin, D. A. Thompson, I. Amit, X. Adiconis, L. Fan,
644 R. Raychowdhury, Q. Zeng, Z. Chen, E. Mauceli, N. Hacohen, A. Gnirke, N. Rhind, F. di Palma,
645 B. W. Birren, C. Nusbaum, K. Lindblad-Toh, N. Friedman and A. Regev (2011). "Full-length
646 transcriptome assembly from RNA-Seq data without a reference genome." Nat Biotechnol
647 **29**(7): 644-652.

648 Hou, Y., H. Lin, L. Zhu, Z. Liu, F. Hu, J. Shi, T. Yang, X. Shi, H. Guo, X. Tan, L. Zhang, Q. Wang, Z.
649 Li and Y. Zhao (2014). "The inhibitory effect of IFN-gamma on protease HTRA1 expression in
650 rheumatoid arthritis." J Immunol **193**(1): 130-138.

651 Ibrahim, A. S., B. Spellberg and J. Edwards, Jr. (2008). "Iron acquisition: a novel perspective on
652 mucormycosis pathogenesis and treatment." Curr Opin Infect Dis **21**(6): 620-625.

653 Inglesfield, S., A. Jasiulewicz, M. Hopwood, J. Tyrrell, G. Youlden, M. Mazon-Moya, O. R.
654 Millington, S. Mostowy, S. Jabbari and K. Voelz (2018). "Robust Phagocyte Recruitment
655 Controls the Opportunistic Fungal Pathogen Mucor circinelloides in Innate Granulomas In
656 Vivo." MBio **9**(2).

657 Itabangi, H., P. Sephton-Clark, X. Zhou, I. Insua, M. Probert, J. Correia, P. Moynihan, T.
658 Gebremariam, Y. Gu, L. Lin, A. S. Ibrahim, G. D. Brown, J. S. King, F. Fernandez Trillo, E. R.
659 Ballou and K. Voelz (2019). "A bacterial endosymbiont enables fungal immune evasion during
660 fatal mucormycete infection " BioRXiv.

661 Kraibooj, K., H. R. Park, H. M. Dahse, C. Skerka, K. Voigt and M. T. Figge (2014). "Virulent strain
662 of Lichtheimia corymbifera shows increased phagocytosis by macrophages as revealed by
663 automated microscopy image analysis." Mycoses **57 Suppl 3**: 56-66.

664 Liu, M., L. Lin, T. Gebremariam, G. Luo, C. D. Skory, S. W. French, T. F. Chou, J. E. Edwards, Jr.
665 and A. S. Ibrahim (2015). "Fob1 and Fob2 Proteins Are Virulence Determinants of Rhizopus
666 oryzae via Facilitating Iron Uptake from Ferrioxamine." PLoS Pathog **11**(5): e1004842.

667 Lorenz, M. C. and G. R. Fink (2001). "The glyoxylate cycle is required for fungal virulence."
668 Nature **412**(6842): 83-86.
669 Luckett-Chastain, L. R., M. L. Cottrell, B. M. Kawar, M. A. Ihnat and R. M. Gallucci (2017).
670 "Interleukin (IL)-6 modulates transforming growth factor-beta receptor I and II (TGF-betaRI
671 and II) function in epidermal keratinocytes." Exp Dermatol **26**(8): 697-704.
672 Ma, L.-J., A. S. Ibrahim, C. Skory, M. G. Grabherr, G. Burger, M. Butler, M. Elias, A. Idnurm, B.
673 F. Lang, T. Sone, A. Abe, S. E. Calvo, L. M. Corrochano, R. Engels, J. Fu, W. Hansberg, J.-M. Kim,
674 C. D. Kodira, M. J. Koehrsen, B. P. Liu, D. Miranda-Saavedra, S. O'leary, L. Ortiz-
675 Castellanos, R. Poulter, J. Rodriguez-Romero, J. Ruiz-Herrera, Y.-Q. Shen, Q. Zeng, J. Galagan,
676 B. W. Birren, C. A. Cuomo and B. L. Wickes (2009). "Genomic Analysis of the Basal Lineage
677 Fungus Rhizopus oryzae Reveals a Whole-Genome Duplication." PLoS genetics **5**(7):
678 e1000549.
679 Martinez, F. O., L. Helming, R. Milde, A. Varin, B. N. Melgert, C. Draijer, B. Thomas, M. Fabbri,
680 A. Crawshaw, L. P. Ho, N. H. Ten Hacken, V. Cobos Jimenez, N. A. Kootstra, J. Hamann, D. R.
681 Greaves, M. Locati, A. Mantovani and S. Gordon (2013). "Genetic programs expressed in
682 resting and IL-4 alternatively activated mouse and human macrophages: similarities and
683 differences." Blood **121**(9): e57-69.
684 Mendoza, L., R. Vilela, K. Voelz, A. S. Ibrahim, K. Voigt and S. C. Lee (2014). "Human Fungal
685 Pathogens of Mucorales and Entomophthorales." Cold Spring Harb Perspect Med **5**(4).
686 Mondo, S. J., O. A. Lastovetsky, M. L. Gaspar, N. H. Schwardt, C. C. Barber, R. Riley, H. Sun, I.
687 V. Grigoriev and T. E. Pawlowska (2017). "Bacterial endosymbionts influence host sexuality
688 and reveal reproductive genes of early divergent fungi." Nat Commun **8**(1): 1843.
689 Mosser, D. M. and X. Zhang (2008). "Activation of murine macrophages." Curr Protoc Immunol
690 **Chapter 14**: Unit 14 12.

691 Muller, C. S., R. Schmaltz, T. Vogt and C. Pfohler (2011). "Expression of CD30 antigen in
692 superficial mycotic infections of the skin: a possible non-specific finding without clinical
693 relevance." Mycoses **54**(5): e360-363.
694 Municio, C., Y. Alvarez, O. Montero, E. Hugo, M. Rodriguez, E. Domingo, S. Alonso, N.
695 Fernandez and M. S. Crespo (2013). "The response of human macrophages to beta-glucans
696 depends on the inflammatory milieu." PLoS One **8**(4): e62016.
697 Munoz, J. F., T. Delorey, C. B. Ford, B. Y. Li, D. A. Thompson, R. P. Rao and C. A. Cuomo (2018).
698 "Coordinated host-pathogen transcriptional dynamics revealed using sorted subpopulations
699 and single, Candida albicans infected macrophages." BioRXiv.
700 Owen, J. L. and M. Mohamadzadeh (2013). "Macrophages and chemokines as mediators of
701 angiogenesis." Front Physiol **4**: 159.
702 Parente-Rocha, J. A., A. F. Parente, L. C. Baeza, S. M. Bonfim, O. Hernandez, J. G. McEwen, A.
703 M. Bailao, C. P. Taborda, C. L. Borges and C. M. Soares (2015). "Macrophage Interaction with
704 Paracoccidioides brasiliensis Yeast Cells Modulates Fungal Metabolism and Generates a
705 Response to Oxidative Stress." PLoS One **10**(9): e0137619.
706 Raggi, F., S. Pelassa, D. Pierobon, F. Penco, M. Gattorno, F. Novelli, A. Eva, L. Varesio, M.
707 Giovarelli and M. C. Bosco (2017). "Regulation of Human Macrophage M1-M2 Polarization
708 Balance by Hypoxia and the Triggering Receptor Expressed on Myeloid Cells-1." Front
709 Immunol **8**: 1097.
710 Robinson, M. D., D. J. McCarthy and G. K. Smyth (2010). "edgeR: a Bioconductor package for
711 differential expression analysis of digital gene expression data." Bioinformatics **26**(1): 139-
712 140.

713 Rogers, H., D. W. Williams, G. J. Feng, M. A. Lewis and X. Q. Wei (2013). "Role of bacterial
714 lipopolysaccharide in enhancing host immune response to Candida albicans." Clin Dev
715 Immunol **2013**: 320168.
716 Schmidt, S., L. Tramsen, S. Perkhofer, C. Lass-Florl, M. Hanisch, F. Roger, T. Klingebiel, U. Koehl
717 and T. Lehrnbecher (2013). "Rhizopus oryzae hyphae are damaged by human natural killer
718 (NK) cells, but suppress NK cell mediated immunity." Immunobiology **218**(7): 939-944.
719 Schroeder, A., O. Mueller, S. Stocker, R. Salowsky, M. Leiber, M. Gassmann, S. Lightfoot, W.
720 Menzel, M. Granzow and T. Ragg (2006). "The RIN: an RNA integrity number for assigning
721 integrity values to RNA measurements." BMC Mol Biol **7**: 3.
722 Sephton-Clark, P. C. S., J. F. Munoz, E. R. Ballou, C. A. Cuomo and K. Voelz (2018). "Pathways
723 of Pathogenicity: Transcriptional Stages of Germination in the Fatal Fungal Pathogen Rhizopus
724 delemar." mSphere **3**(5).
725 Shen, Q., M. J. Beucler, S. C. Ray and C. A. Rappleye (2018). "Macrophage activation by IFN-
726 gamma triggers restriction of phagosomal copper from intracellular pathogens." PLoS Pathog
727 **14**(11): e1007444.
728 Spellberg, B., J. Edwards, Jr. and A. Ibrahim (2005). "Novel perspectives on mucormycosis:
729 pathophysiology, presentation, and management." Clin Microbiol Rev **18**(3): 556-569.
730 Szulzewsky, F., A. Pelz, X. Feng, M. Synowitz, D. Markovic, T. Langmann, I. R. Holtman, X.
731 Wang, B. J. Eggen, H. W. Boddeke, D. Hambardzumyan, S. A. Wolf and H. Kettenmann (2015).
732 "Glioma-associated microglia/macrophages display an expression profile different from M1
733 and M2 polarization and highly express Gpnmb and Spp1." PLoS One **10**(2): e0116644.
734 van Tol, S., A. Hage, M. I. Giraldo, P. Bharaj and R. Rajsbaum (2017). "The TRIMendous Role
735 of TRIMs in Virus-Host Interactions." Vaccines (Basel) **5**(3).

736 Warris, A., M. G. Netea, P. E. Verweij, P. Gaustad, B. J. Kullberg, C. M. Weemaes and T. G.
737 Abrahamsen (2005). "Cytokine responses and regulation of interferon-gamma release by
738 human mononuclear cells to Aspergillus fumigatus and other filamentous fungi." Med Mycol
739 **43**(7): 613-621.
740 Yadav, A. K., P. R. Desai, M. N. Rai, R. Kaur, K. Ganesan and A. K. Bachhawat (2011).
741 "Glutathione biosynthesis in the yeast pathogens Candida glabrata and Candida albicans:
742 essential in C. glabrata, and essential for virulence in C. albicans." Microbiology **157**(Pt 2): 484-
743 495.
744 Ye, R. D. and L. Sun (2015). "Emerging functions of serum amyloid A in inflammation." J Leukoc
745 Biol **98**(6): 923-929.
746

747

748 **Figure legends**

749 **Figure 1 Phenotypic and genomic comparisons.** A) Experimental setup: Pre-swollen (SAB)
750 wild-type (wt) or cured fungal spores from *Rhizopus delemar* (2hr) and *Rhizopus microsporus*
751 (4hr) in mid-isotropic phase were co-cultured with J774.1 murine macrophages (sfDMEM) at
752 5:1 MOI for 1hr, washed to remove unengulfed spores, then co-incubated for a further 2
753 hours before fungi and host cells were harvested. Pre-swollen spores (SAB) incubated in
754 sfDMEM for 3hr served as the negative control. B) Germination percentage over time for *R.*
755 *delemar* and *R. microsporus* grown in SAB. C) Spore sizes for *R. delemar* and *R. microsporus*
756 grown in SAB. D) Pfam terms enriched (corrected $P < 0.01$) in *R. delemar* vs *R. microsporus*
757 genomes, with colour indicating the extent of enrichment ($Log_{10}$ Count).

758 **Figure 2 Principal component analysis of fungal genes differentially expressed across all**

759 **samples.** A) *R. delemar* wt and cured, macrophage engulfed or sfDMEM control B) *R.*
760 *microsporus* wt and cured, macrophage engulfed or sfDMEM control. Biological replicates
761 (n=3) are shown for each sample.

762 **Figure 3 Clustering of fungal transcriptional changes.** A) Heatmap displaying differentially
763 expressed genes in *R. delemar*. Expression levels are plotted in Log2, space and mean-
764 centered (FDR < 0.001) B) Heatmap displaying differentially expressed genes in *R.*
765 *microsporus*. Expression levels are plotted in Log2, space and mean-centered (FDR < 0.001).

766 **Figure 4 Differential expression of fungal genes in compared conditions**. A) The number of
767 genes significantly differentially expressed (multiple corrected P value < 0.05) between
768 samples. Blue bars indicate genes with an increase in expression (LogFC > 2), whilst orange
769 bars indicate genes with a decrease in expression (LogFC < -2).

770 **Figure 5 Functions of genes differentially expressed in *R. delemar*.** Enriched KEGG categories
771 for the up/down (LogFC > 2 or < -2) regulated genes over sample comparisons. The
772 enrichment of the category is indicated by the colour bar. White corresponds to no
773 enrichment, and yellow to red corresponds to the given P value of the enrichment.

774 **Figure 6 Principal component analysis of macrophage genes differentially expressed across**
775 **all samples.** Single cell sequencing was performed on uninfected and infected macrophages.
776 Transcriptional data from the experiment was analysed with the 10X genomics analysis
777 pipeline, and aggregated prior to principle component analysis.

778 **Figure 7 Clustering of macrophage transcription.** Heatmap displaying immune response
779 genes significantly differentially expressed between aggregated macrophage populations.
780 Expression levels are plotted in Log2 (FDR < 0.001)

781 **Figure 8 Macrophage survival following exposure to *R. delemar* and *R. microsporus* spores.**
782 Macrophages +/- LPS pre-treatment were infected (MOI 5:1) with fungal spores, pre-swollen
783 in SAB consistent with transcriptional experiments. Macrophages were infected with fungal
784 spores that were pre-treated with +/- Nikkomycin Z (24 μg/ml; biological replicate n=3 for
785 each sample). Macrophage survival was determined 7 hr post infection. Significant
786 differences between samples is indicated by (*= $p < 0.01$). 3 biological replicates per
787 condition.

788 **Supplemental Figure 1** Table of Pfam terms found to be enriched (corrected $P < 5 \times 10^{-8}$) in *R.*
789 *delemar* and *R. microsporus* upon genome comparison.

790 **Supplemental Figure 2 Clustering of fungal transcription with GO annotation**. Heatmap
791 displaying all differentially expressed genes, across all conditions, in *R. microsporus*.
792 Expression levels are plotted in Log2, space and mean-centered (FDR < 0.001). GeneIDs
793 correspond to the genome of *Rhizopus microsporus* (ATCC 52813, accession:
794 GCA_002708625.1)

795 **Supplemental Figure 3 *Ralstonia picketti* expression.** Volcano plot highlighting significantly
796 (red, FDR < 0.0001) differentially expressed genes from *Ralstonia picketti* grown in DMEM vs
797 DMEM supplemented with *R. microsporus* substrate. Labelled genes show a LogFC ± 2
798 between these two conditions. Gene IDs refer to the *R. pickettii* 12J reference genome.
799

800 **Supplemental Figure 4 DEGs and clustering of J774.1 macrophages**. A) Principal component
801 analysis of single cells based on significantly differentially expressed genes (top), and immune
802 response genes (bottom). B) Gene counts per million (Log10(CPM+1)) for all genes
803 differentially expressed (adjusted p value < 0.0001), per cell, with genes falling into enriched

804 functions labelled by colour. 1082 single cells spanning all conditions represented.

805 **Supplemental Figure 5 Expression of chitin synthase genes**. A) Heatmap showing the
806 expression of chitin synthase genes in *R. delemar.* B) Heatmap showing the expression of
807 chitin synthase genes in *R. microsporus.*

808 **Supplemental Figure 6 Chitin synthase inhibition of *R. delemar* and *R. microsporus***
809 **germination**. *R. delemar* and *R. microsporus* treated with Nikkomycin Z in SAB at indicated
810 concentrations. Fluorescence indicates calcofluor white staining, and thus the availability of
811 chitin/chitosan in the cell wall.

812 **Supplemental Table 1** Selected genes differentially regulated in pairwise comparisons, with
813 Pfam annotations provided where available.

814 **Supplemental Table 2** Table displaying the LogFC values for a subset of genes displayed in
815 Figure 7.

816 **Supplemental Table 3** Table displaying genes differentially expressed by *R. delemar* (2,493),
817 as displayed in Figure 3a.

818

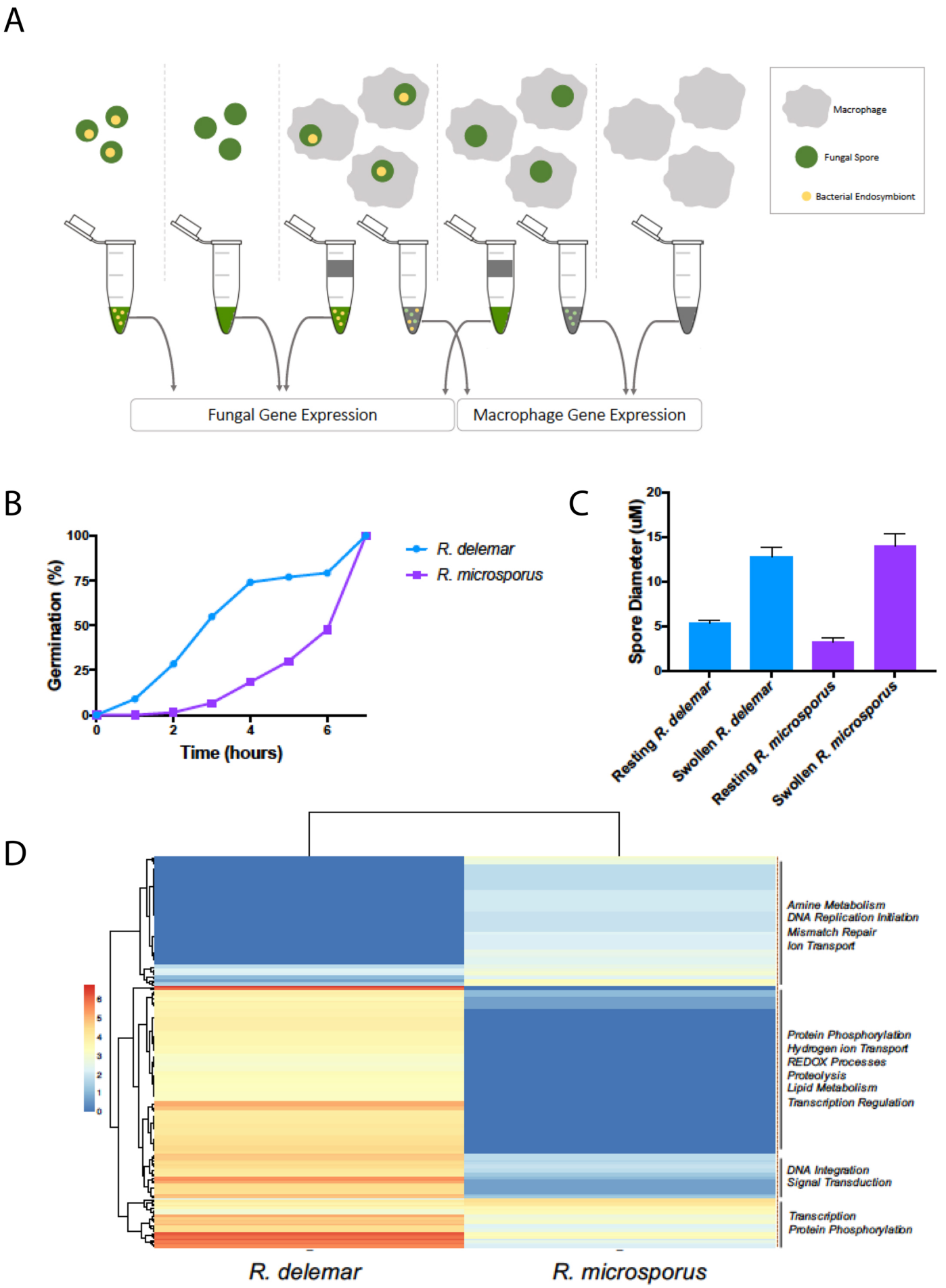


Figure 1 Phenotypic and genomic comparisons. A) Experimental setup: Pre-swollen (SAB) wild-type (wt) or cured fungal spores from Rhizopus delemar (2hr) and Rhizopus microsporus (4hr) in mid-isotropic phase were co-cultured with J774.1 murine macrophages (sfDMEM) at 5:1 MOI for 1hr, washed to remove unengulfed spores, then co-incubated for a further 2 hours before fungi and host cells were harvested. Pre-swollen spores (SAB) incubated in sfDMEM for 3hr served as the negative control. B) Germination percentage over time for R. delemar and R. microsporus grown in SAB. C) Spore sizes for R. delemar and R. microsporus grown in SAB. D) Pfam terms enriched (corrected $P < 0.01$) in R. delemar vs R. microsporus genomes, with colour indicating the extent of enrichment (Log10 Count).

Figure 2

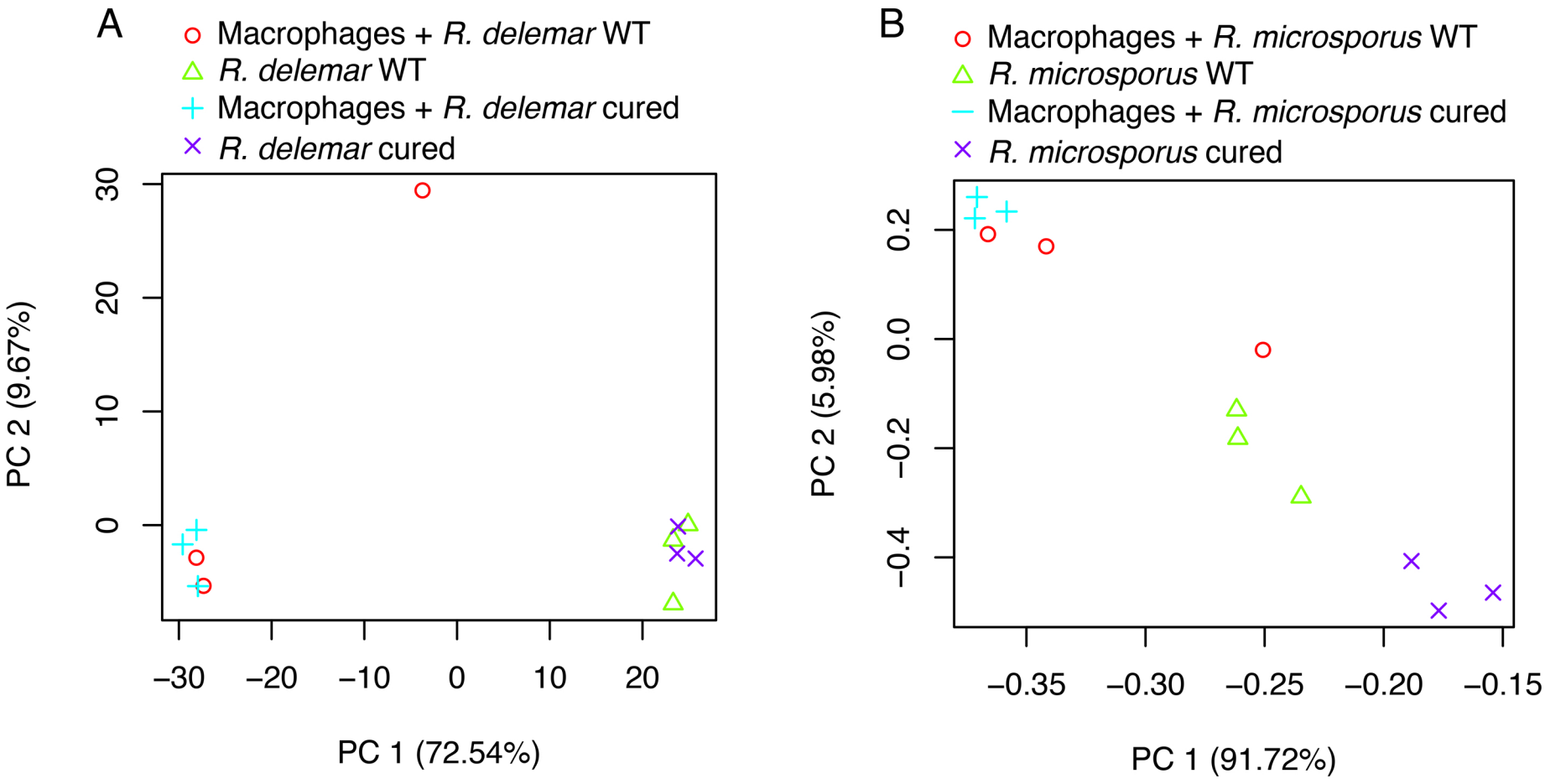


Figure 2 Principal component analysis of fungal genes differentially expressed across all samples. A) R. delemar wt and cured, macrophage engulfed or sfDMEM control B) R. microsporus wt and cured, macrophage engulfed or sfDMEM control. Biological replicates (n=3) are shown for each sample.

Figure 3

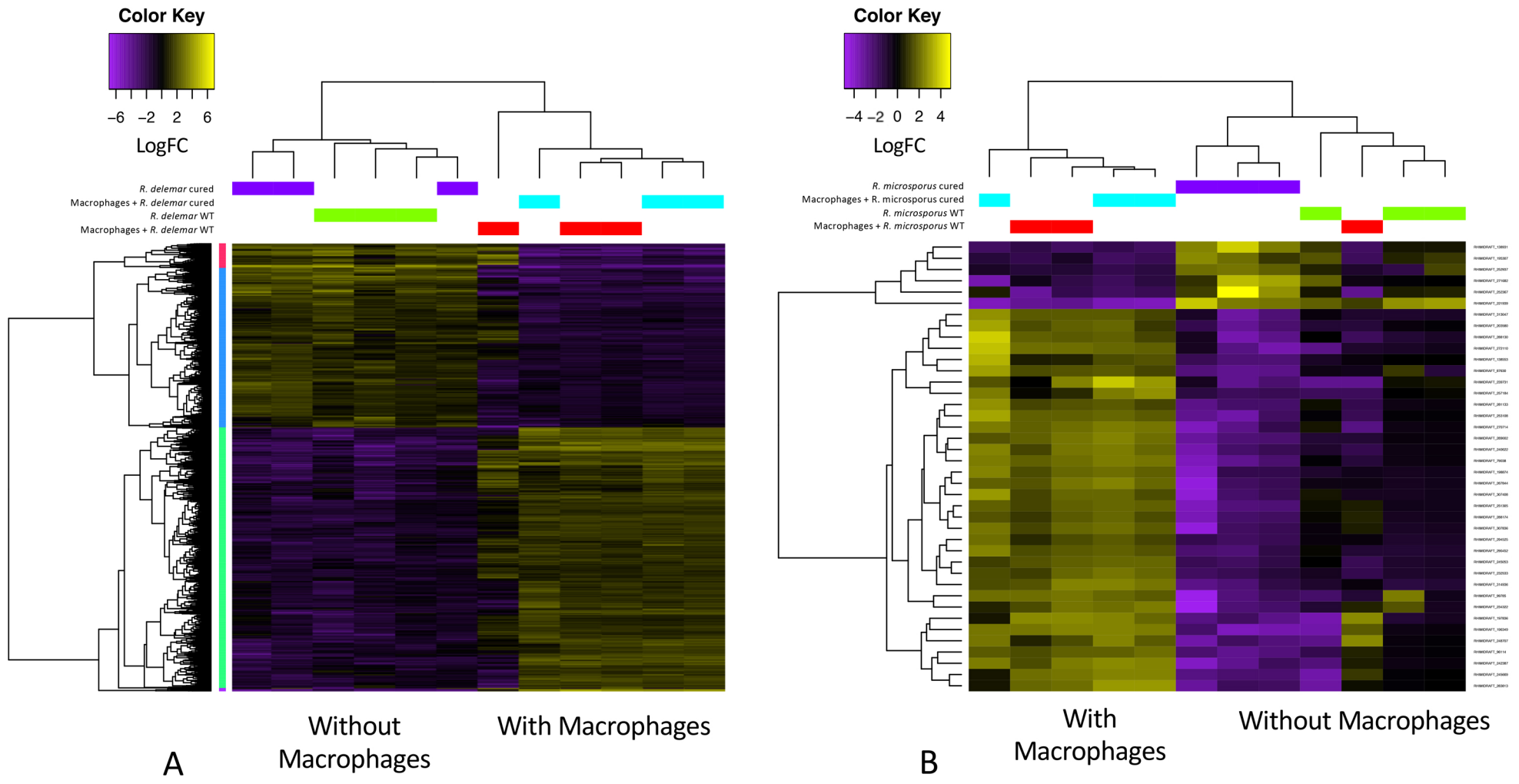


Figure 3 Clustering of fungal transcriptional changes. A) Heatmap displaying differentially expressed genes in R. delemar. Expression levels are plotted in Log2, space and mean-centered (FDR < 0.001) B) Heatmap displaying differentially expressed genes in R. microsporus. Expression levels are plotted in Log2, space and mean-centered (FDR < 0.001).

Figure 4

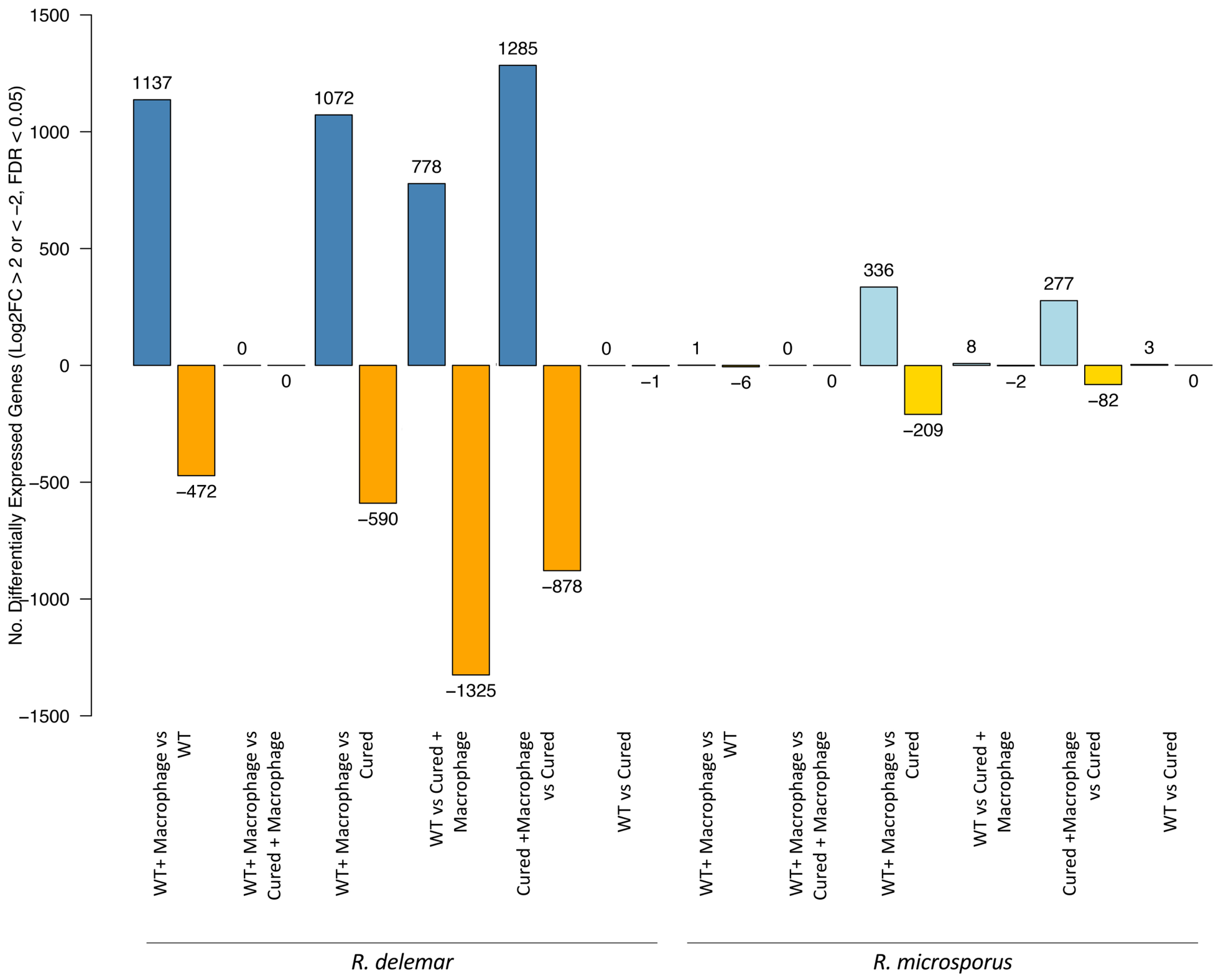


Figure 4 Differential expression of fungal genes in compared conditions. A) The number of genes significantly differentially expressed (multiple corrected P value < 0.05) between samples. Blue bars indicate genes with an increase in expression (LogFC > 2), whilst orange bars indicate genes with a decrease in expression (LogFC < -2).

Figure 5

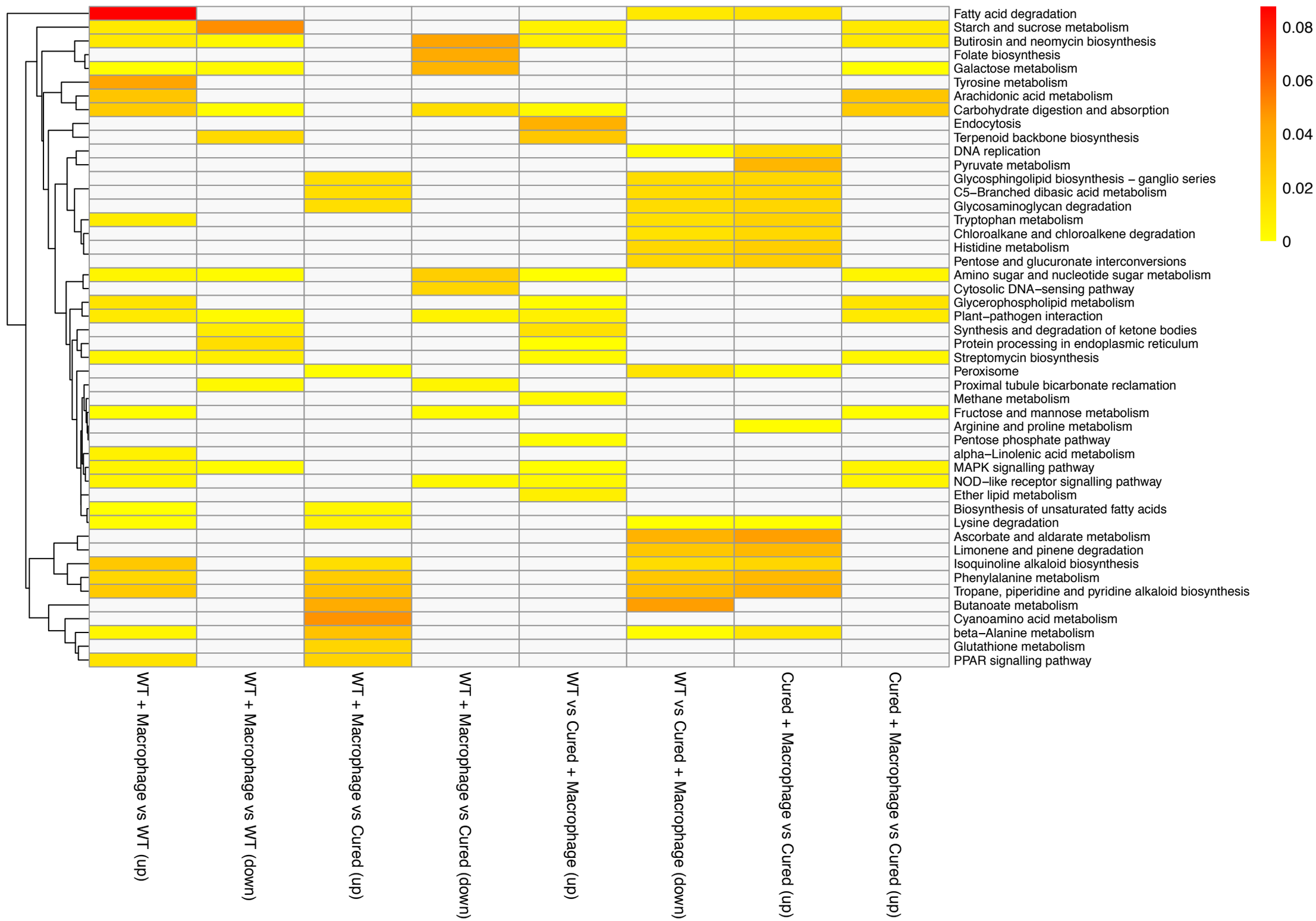


Figure 5 Functions of genes differentially expressed in R. delemar. Enriched KEGG categories for the up/down (LogFC > 2 or < -2) regulated genes over sample comparisons. The enrichment of the category is indicated by the colour bar. White corresponds to no enrichment, and yellow to red corresponds to the given P value of the enrichment.

Figure 6

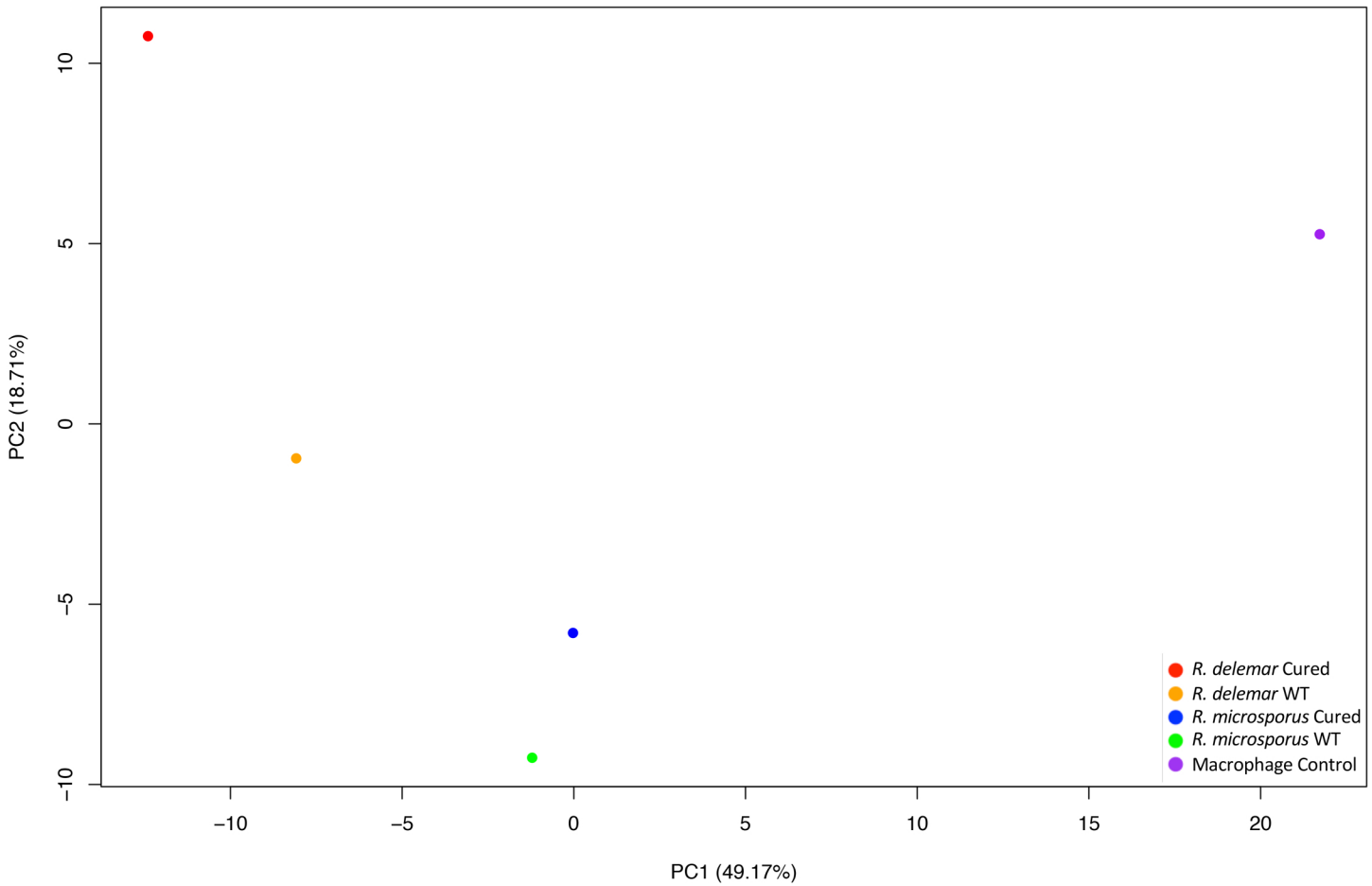


Figure 6 Principal component analysis of macrophage genes differentially expressed across all samples. Single cell sequencing was performed on uninfected and infected macrophages. Transcriptional data from the experiment was analysed with the 10X genomics analysis pipeline, and aggregated prior to principle component analysis.

Figure 7

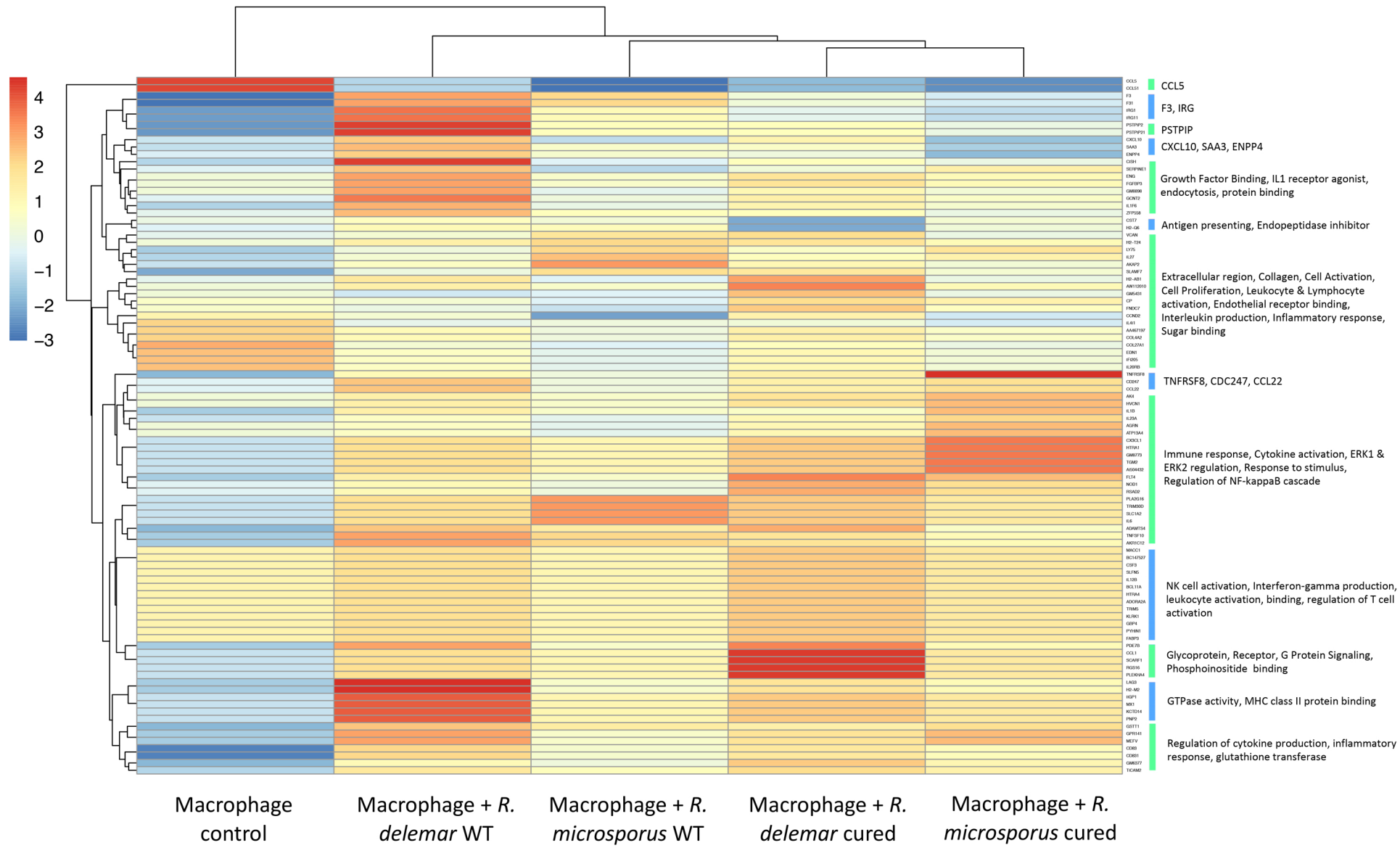


Figure 7 Clustering of macrophage transcription. Heatmap displaying immune response genes significantly differentially expressed between aggregated macrophage populations. Expression levels are plotted in Log2 (FDR < 0.001)

Figure 8

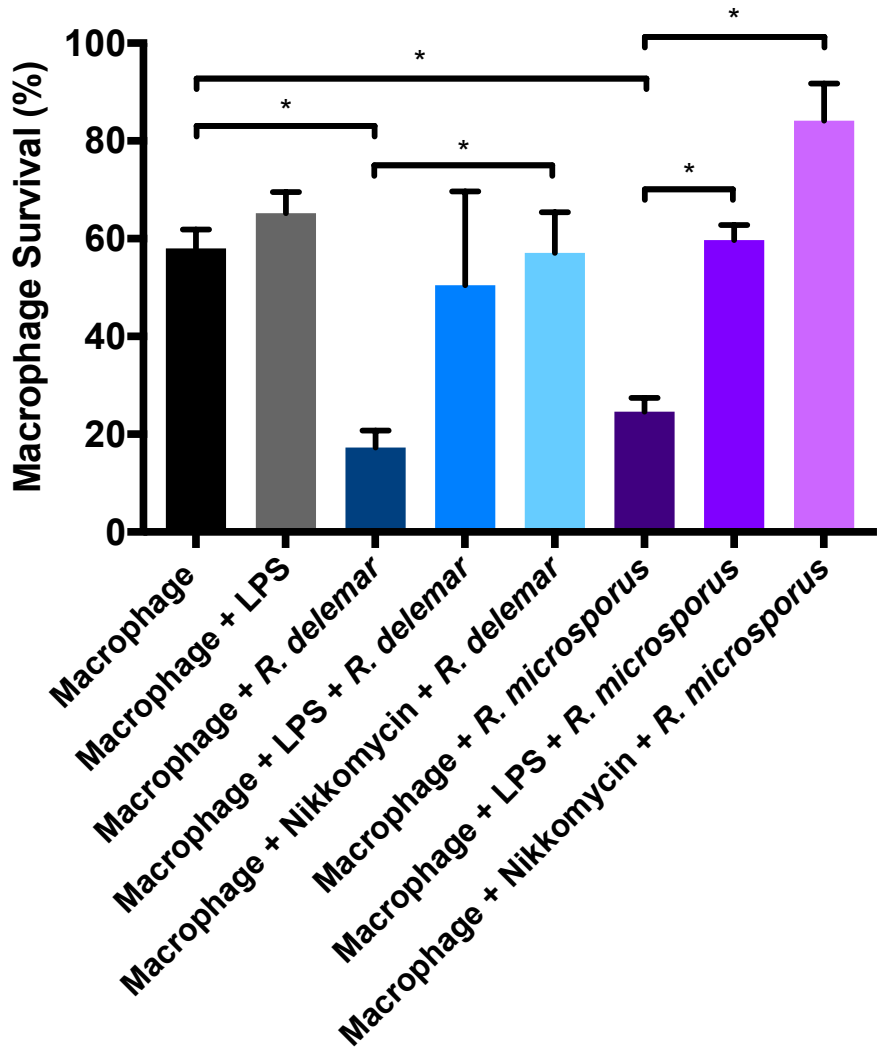


Figure 8 Macrophage survival following exposure to R. delemar and R. microsporus spores. Macrophages +/- LPS pre-treatment were infected (MOI 5:1) with fungal spores, pre-swollen in SAB consistent with transcriptional experiments. Macrophages were infected with fungal spores that were pre-treated with +/- Nikkomycin Z (24 g/ml; biological replicate n=3 for each sample). Macrophage survival was determined 7 hr post infection. Significant differences between samples is indicated by (*= $p < 0.01$). 3 biological replicates per condition.